# Analysis of a Hydrogen Flying Airplane

De Aguiar, João B[1], Tacksian, Isadora F.[2] De Aguiar, José M.[3]

[1,2]*Engenharia Aeroespacial, UFABC*
*Av. dos Estados,5001, Bangu, 09210-580, Santo André, SP, Brazil*
*joao,aguiar@ufabc.edu.br*
[2]*Ensino Geral, FATEC-SP*
*Av. Tiradentes, 615, Bom Retiro, 01101-010, São Paulo, SP, Brazil*
*josemaguiar@gmail.com*

**Abstract.** Present aircrafts make use of fossil fuels in combustion processes that create large amounts of emissions. Pollution and climate changes are perceived as related to this type of emissions. These worries have led to worldwide efforts towards reduction in the use of combustion engines. Clean airplanes with zero direct emissions require technological developments some yet in exploratory phase. Hydrogen propelled airplanes promise large reductions in $CO_2$ emissions. Design, testing and evaluation of power type modified airplanes is quite challenging, as a whole new system of components is required to work with the fuel cell. To this endeavor a method is presented here, with parameters from a conceptual plane chosen as reference airplane, so as to avoid unnecessary and costly changes. Once verified the main premises, structural response of the hydrogen powered airplane is developed with due consideration of powertrain components. For the plane, the same mission requirements are set. Balance of the plant is undertaken, before specifications are done. A first order structural analysis of the plane, for cruise conditions, shows redundancy enough to accept the modifications. Discussion and comparisons are presented.

**Keywords:** Hydrogen plane, balance of plant, redesign, analysis

## 1. Introduction

Airplanes burning fossil fuels, like kerosene, create large amounts of heat that it is believed to contribute to the overall climate change. Creation and protection of present forests is a deterrent to this problem. Use of alternative fuels to power flying machines is another. Clearly pollution problems are aggravated by use of internal combustion engines, even if the heat problem is controlled. As the best solution is yet unknown, a great amount of effort is devoted nowadays towards having a cleaner aviation. Aviation contributes to about 4% of global warming.

Many alternative propulsive machines have been proposed to meliorate this problem so far. Among them the ones using electric motors, with energy coming from solar panels, hydrogen fuel cells, or some other gas, as well as hybrid engines, are some of the list. Conceptual and preliminary designs for some of these solutions are available in the technical literature [1]-[4], albeit the fact that most consider only source and powertrain modifications of existing airplanes. This is so because the technology in this area is changing fast, and many unsatisfactory results were obtained with new designs. The exchange of the propulsion system, with the modifications accompanying it, is then a first step towards an evaluation of the solution. It is the procedure used in the work.

Small and commuter airplanes are considered the best fit to be powered by stacks of hydrogen fuel cells. Airplanes in these categories use single engines or multiple engines, lower speeds and small a few passengers. Some carry only the pilot, as is the case of PIK 26. This airplane is special because of its simplicity what turn it preferred as a research plane, Fig. 1. It will be used here to unveil the some of the effects of change when a hydrogen fuel cell is installed in it.

PIK 26 Mini-Sytky is a low-wing monoplane, designed by the Finnish aircraft designer Kai Mellen. Its high performance allows it to cruise at 173 km/h, category B, while burning gasoline at a rate of 7 liters/hour. Several aircraft of this design fly worldwide. The PIK-26 is mainly constructed from wood. While the skins are made of birch plywood, and the spars of pine, the wing ribs are made of PVC foam. As a personal airplane, construction plans are offered for free in the internet, with an estimated construction time of about 2,300 hours [2].


Figure 1: PIK 26 photo

Table 1. Some characteristics of PIK 26 wings

| Parameter | Value |
|---|---|
| Length,m | 5.24 |
| Chord, m | 1.14 |
| Taper ratio | 1.0 |
| Wing area,m2 | 6.0 |
| Horizontal tail aspect ratio | 5.0 |
| Vertical tail aspect ratio | 5.0 |

## 2. Concept, Model and Analysis

Currently there are prototypes of hydrogen fuel cell aircrafts in testing, but not enough data is available for comparison. Therefore, instead of developing a conceptual and preliminary design of a new airplane, here a reference airplane will have its generation and powertrain based on a fossil fuel, exchanged by a complete hydrogen fuel cell. This work will allow understanding the most important facts to deal when developing a particular solution specific to hydrogen powering.

### 2.1 Reference Airplane

Some performance parameters of PIK 26 are presented in the Table 2. They reveal the elements needed in the characterization of the behavior of the airplane when burning gasoline. They allow determination of the behavior of the airplane in the diverse phases of flight, and constitute the mission requirements. These will serve as guidelines to the requested response of the airplane when the internal combustion engine and powertrain are

substituted by a stack of hydrogen fuel cells, with auxiliary elements battery, tank and electrical motor. Flight performance, involving the typical phases of it – takeoff, climbing, turn, level flight and descent – has to be established, prior and after the power source is changed.

Table 2. Main characteristics of PIK-26

| Parameter | Value |
|---|---|
| Harmonic range, km | 450 |
| Cruise speed, km/h | 170 |
| Climb speed. m/s | 3.2 |
| Takeoff speed, m/s | 28 |
| Sustained turning speed | 20 |
| Sea level rate of climb | 9 |
| Service ceiling, m | 3300 |
| Stall speed, km/h | 63 |
| Takeoff roll distance, m | 170 |
| Cruise altitude, m | 2000 |
| Payload mass, kg | 106 |

For a takeoff on a runway at sea level with mild temperatures – $20^0$C –no winds, starting at initial zero velocity, with weight $W_{to} = m_{to} g$ , vertical force components equated, under constant acceleration give:

$$T_{to} = W[\frac{v_{to}^{\ 2}}{2gs_o} + q_{to} C_{Dy_0} (W/S)^{-1} + \mu(1 - q_{to} C_{L\,to} (W/S)^{-1})] \tag{1}$$

Here $S$ is the wing area, $C_D$ and $C_L$ are the drag and lift coefficients. These coefficients are defined from the angle of attack set in the takeoff. The response of the GAW airfoil – NACA LS-0412-ls - at 1e6 Reynolds number may be obtained from XFBR5 [5] and use as an estimate. For a takeoff angle of attach of 12 $^{O}$, these coefficients are 0.02541 and 1.6388, respectively. Takeoff mass is obtained by adding the empty airplane mass $m_e$ with the payload $m_p$ . The trust is $T_{to}$ , the dynamic pressure is $q_{to} = \frac{\rho}{2} V^2$ and wing pressure is $W_{to} / S$ . Roll distance is $s_0$ and pavement frictional coefficient is\ $\mu$ .

Following takeoff, the airplane climbs at high power in search of required flight altitude. This part of the trajectory is described by:

$$T_v = W_v[C_{D_v} q_v (W_v / S)^{-1} + k q_v^{\ -1} (W_v / S)] \tag{2}$$

Coefficients depend on the angle of attack considered. Weight is approximately the same. Here $k = (\pi e AR)^{-1}$ with $AR = b^2 S^{-2}$ stands for aspect ratio. The amount of thrust stays close to the maximum. From this phase on, normally some turn takes place in search for level flight. This sector of the trajectory is described in the following manner:

$$T_t = W_t[C_{D_t} q_t (W_r / S)^{-1} + q_t^{=2} n^2 k (W_r / S)] \tag{3}$$

where $n$ stands for the g-number occurring in the turn. Radius $R$ is required here.

Next level flight takes place and another value of thrust is required, computed from an angle of incidence $\alpha_c$ at cruise. Several settings are possible here, according to the height $h_c$ and velocity Horizontal equilibrium requires that:

$$T_c = W_c[C_{D_c} q_c (W_c / S)^{-1} + k q_c^{\ -1} (W_c / S)] \tag{4}$$

Final sector in a flight obeys similar equation to takeoff, Eq. (1). In general, a different distance in contact with

pavement is used, however, $s_{lan}$ .A part this set of equations, a maximum ceiling occurs $h_M$ , and a minimum velocity, the stall speed:

$$v_s = \sqrt{\frac{2W_s}{\rho_s S C_{L_s}}} \tag{5}$$

Being the lift coefficient computed at maximum.

### 2.2 Hydrogen Fuel Plant

One form of powering a PIK 26 consists in having a 35 hp engine installed. In such an engine, gasoline is burned. Some systems are required for proper functioning of this engine. They comprise an admission system with air entrance at front, filter and flow meter. Probes are used in this admission line to measure temperature, pressure and humidity. Better engine performance is possible if enriched air is used. This may be obtained with the coupling of a compressor to this line. A humidifier is a plus. Excess air return passages are also present in some solutions, and a pass valve. Power required to operate the admission line is $\dot{W}_{air}$ .

The other inflow line takes the fuel from a tank to the engine throttle by means of a pump. In this line, filter, probes, meters and most of the other elements of the air intake are present. Control on the quality of the mixture air-fuel may be mechanical or electronic. This parallel line requires power as well, $\dot{W}_{fuel}$

Admission and exhaust valves in the engine control access to the combustion chamber. The amount of energy used depends on the number of cylinders, running velocity and internal losses of the mechanical elements. Here another amount of energy $\dot{W}_{valve}$ is required. In complement, cooling and lubrication systems are needed for proper working of the engine. Corresponding amounts of energy for these systems are $\dot{W}_{coo;}$ and $\dot{W}_{\text{lub}}$ . The sum of all these power elements is $\dot{W}_{parasitic}$ , the parasitic power. This amount of energy comes from the generated in the internal combustion engine to render the net power, $\dot{W}_{net} = \dot{W}_{eng} - \dot{W}_{parasitic}$ .

When the power unit of the PIK 26 is substituted by a proton exchange hydrogen unit, similar systems are needed, with emphasis in a higher pressure hydrogen tank. Many of these tanks operate at 700 bar pressures, being built of composite materials. This unit operates with less auxiliary systems, as the valve and lubricant systems are not required as no combustion takes place. In each cell of the unit, hydrogen reaches the anode, being decomposed there as:

$$1H_2 \Leftrightarrow 2H^+ + 2e^- \tag{6}$$

With the electrons being separated from the hydrogen. At the other side, the cathode receives the oxygen that gathers the electrons coming externally from the other side:

$$\frac{1}{2}O_2 + 2e^- \Leftrightarrow O^{s-} \tag{7}$$

so that, upon adding equations,

$$H_2 + \frac{1}{2}O_2 \Leftrightarrow H_2O + \Delta E \tag{8}$$

The hydrogen protons cross the catalytic membrane inside the cell, after separation from the electrons, coming to reach the other side where they will combine with oxygen ions to generate water. The reaction is exothermal, with some energy coming out from the process. This energy will be stored in a battery. The heat will require a cooling system.

The air inlet line may be represented schematically as in Figure 2. The inlet conditions require inlet temperature $T_i$ and air pressure $p_i$ , each one with an accompanying variation interval. In this line most of the energy is used to power a compressor, used to enrich the air, allowing more oxygen to be extracted.

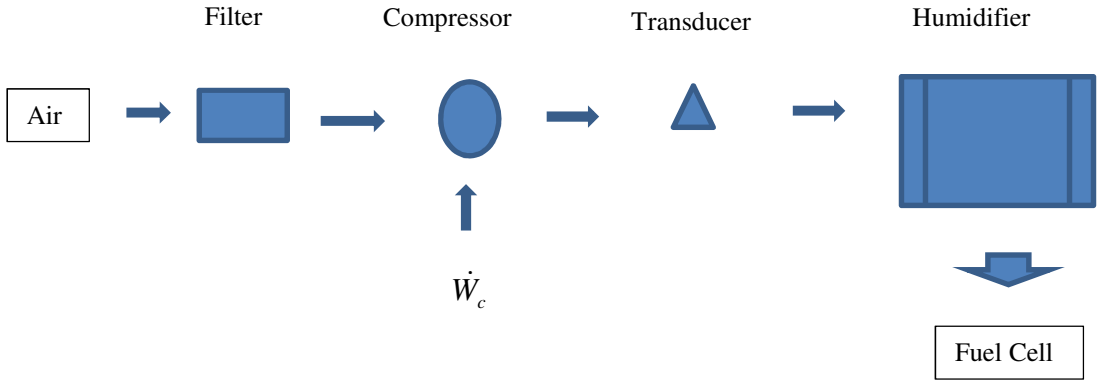


Figure 2. Schematics of air intake line

The most important item in this admission line is the compressor. In some circumstances a heat exchanger is also present. For the compressor, energy conservation requires:

$$\dot{W}_c = \dot{m}_{air}(h_o - h_i) \tag{9}$$

where the air flow is established by the stoichiometric relations in the fuel cell equation. The inflow enthalpy $h_i$ is determined from the intake pressure and temperature. Isotropic adiabatic conditions $s_i = s_0$ are supposed. Prescribing the operational pressure required at the cell stack $p_0 = p_{cell}$ completes the computation.

The hydrogen influx line has schematics starting at the hydrogen tank, kept at $T_i'$ and pressure $p_i'$ parameters prescribed, as well as the mass flow of hydrogen $\dot{m}_{hydrogen}$, based on stoichiometry. Probes are used to measure and keep track of these quantities. A pressure reduction valve is used at the outlet point from tank, to meet the cell requirements. The schematics of the hydrogen line includes, in some versions, purifiers, and a return path for the excess of hydrogen, Fig 3.

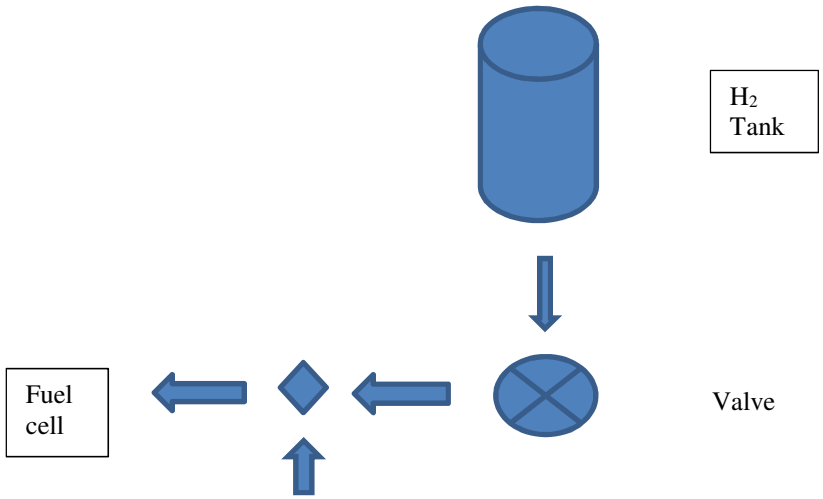


**Figure 3: Hydrogen supply line schematics**

For the valve in this line, enthalpy at exit of hydrogen $h_i'$ is obtained from conditions at the tank. At the exit, conditions depend on the prescribed operational pressure of the cell $p_o'$. Temperature is obtained from use of a control volume around the valve:

$$\dot{Q}_v = \dot{W}_v + \dot{m}_h(h_o' - h_i') \tag{10}$$

with constancy of enthalpy with irreversible work and heat.

As the stack of cells produce a considerable amount of heat, part of which is present in the exhaust water, and some in the excess of hydrogen and air. This excess of heat has to be extracted from the stack. A parallel cooling line is then required, In this line, a cooling water mass flow, $\dot{m}_{cool}$ exiting the cell at temperature $T_i^*$ and pressure $p_i^*$ crosses with incoming air $\dot{m}_{air}^*$ at the intake conditions. It takes place inside a heat exchanger. With no pressure modifications and knowing the temperature of operation of the cell stack, energy conservation on a control volume around the heat exchanger shows that:

$$\dot{m}_{cool}^* (h_c^* - h_{op}) = \dot{m}_{air}^* (h_i - h_0^*) \tag{11}$$

With these elements compressor, pump and heat exchanger, as well other components of the system may be specified.

### 2.3 Modified Plane Performance

PIK 26 is, normally equipped with a Citroen Visa engine of 4 cylinders of 652 cm$^3$ – piston diameter $\phi = 770$ mm and stroke $l = 70$ mm, 4 valves, with a compression ratio of 9:1, delivering 47 Nm at 3500 rpm. Its power values 34.5 hp at 5500 rpm. The mass of the engine is about 45 kg. Transmission may add 20% to this value.

The use of a hydrogen fuel to power the airplane requires specification of a system of at least 40KW, circa of 53 hp nominal, more than 53 KW at the stack, due to the increase of mass of the whole powertrain [7]. Typically a hydrogen fuel cell of this size weights presently around 140 kg. Computation of power requirements of the various systems adds to more than 3 hp, which is the power expanded as parasitic power. Conditions of operation in mild climate, as present in Brazil, have been taken. They are used in most regional flights in the country.

The above expressions, Eqs. (9) up to (11), were used in the balance of the plant to ascertain the range of required power for operation of the air and hydrogen intake lines. It was supposed a 150% oversupply of oxygen for better performance of the cell, supposed to operate on a 1.2 bar pressure, and a temperature range of +-20$^0$C over the average. Electrical current produced from the stack of 200 cells is around 400@132 V, with boost to 600V. Stack consumes circa 0.6 m3$H_2$/KWh. A tank of 125 l for the proposed range would weight 150 kg.

Under these assumptions, power expenditures in every of the flight sectors, for the gasoline and hydrogen powered airplane were compared. An increase in mass of the powertrain and generation unit, was consistently obtained for diverse configurations. A 50% fuel cell performance, consistent with used values nowadays, in normal current densities for the cells, was supposed. To the empty mass of the airplane $m_e = 144$ kg, after the internal combustion engine system was taken out, the mass of the new components was added. More than 100% increase in mass was obtained, $m_t + \Delta m_t = 638$ kg, included here the $m_p = 79$ kg, luggage $m_l = 5$ kg, electrical motor $m_m = 170$ kg and tank. Without sacrificing the payload, a heavier plane with about 65 % more power was required. The weight of the hydrogen tanks for the same mission range, with the difference in consumption, was an important element for this increase in mass and expenditure. The efficiency of the simpler transmission system used with hydrogen fuel is important.

Once an installation was specified each and every stretch of the normal flight, as present in equations (1) up to (5) were compared. Mission requirements were satisfied, but in general with lower velocities, making the time to complete the range flight higher.

### 2.4 Finite Element Model

A drawing of the reference airplane PIK 26 was produced with the program Nastran$^{TM}$. Aside the flow characteristics of the airplane, its structural response is required. Therefore a model of its structure was constructed. Main dimensions, forms and profiles were used in it. Table 3 shows material properties of balsa wood, pine and polyurethane employed in the construction of the airplane. In Fig. 4, the frame required for the structural analysis of the airplane is shown. Discretization of the structure required use of shell elements to assure some level of quality in the description of the displacement field, for individual part analyses, and global analysis. Elasticity was assumed throughout. Reason why Mises, Tsai-Hill and Tsai-Wu criteria were used.

Table 3. Elastic Material Properties

| Material | Elasticity Modulus | Poisson's ratio |
|---|---|---|
| Pine | 20e+09 | 0.20 |
| Balsa Wood | 10e+09 | 0.18 |
| PVC Foam | 3.e+09 | 0.40 |
| Steel | 200.e+09 | 0.30 |

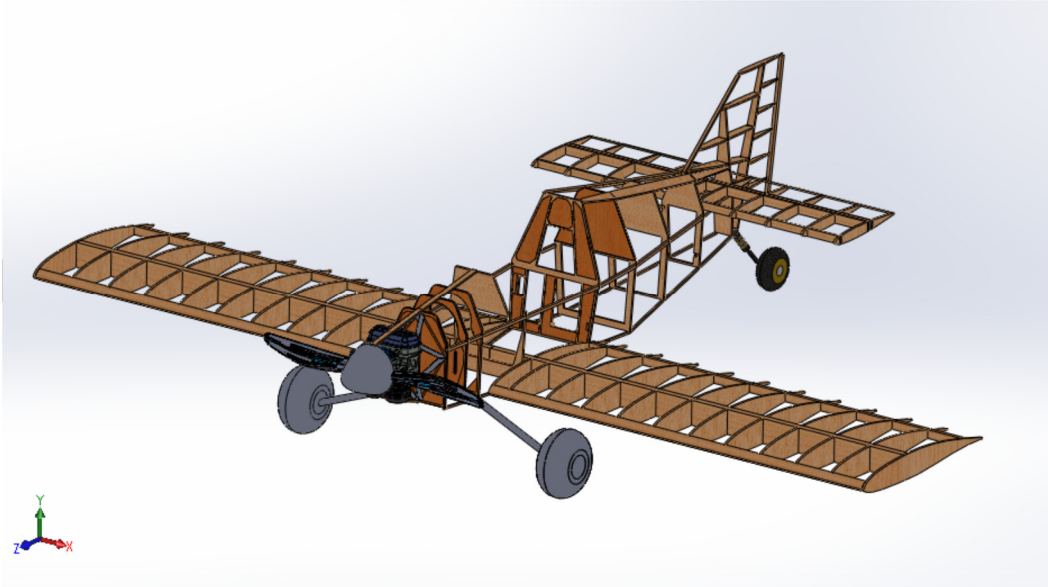

Figure 4. Frame model of PIK 26

As most of the flight occurs at level flight, this condition is used in the load prescription used in the analysis. Wings are responsible for carrying the lifting resultant $L_w$ caused by pressure difference between lower and upper wing surfaces. This resultant per unit length has an elliptic distribution. Here a uniform distribution, which results in higher bending, is used. In doing so, uniform load in each airfoil GAW 2 turns out. These profiles are supported by a spar. Leading and trailing edge complete the wing frame. Only a small part of the lift is supported by the rear wings $L_e$ the empennage. The total lift force, at constant cruise velocity, balances the weight of the airplane. Distribution of this weight depends on the elements of transmission and power generation.

Longitudinal drag is applied mostly at the fuselage of the airplane. It appears as shear in the skin that covers the fuselage. In the frame model, load of every panel is transferred to the basic frame of fuselage, being supported by longitudinal and transverse parts. This drag is balanced by the thrust force, in between propeller and gear box. Lateral shear and bending moments arising at the region of fixation of the wing are present as well.

Principle of virtual work applied to the frame requires that internal and external virtual contributions equal each other;

$$\int_V \delta\boldsymbol{\varepsilon}^T \boldsymbol{\sigma}\, dV = \int_L \delta\mathbf{d}^T \mathbf{l}\, dl \tag{12}$$

In the elastic range, the Cauchy stress tensor $\boldsymbol{\sigma}$ may be written in terms of strains $\boldsymbol{\varepsilon}$ by means of a constitutive tensor $\mathbf{C}$ so that $\boldsymbol{\sigma} = \mathbf{C} :: \boldsymbol{\varepsilon}$. Different materials have distinct elastic parameters $< E, \nu >$.

Upon discretization of the structure into finite elements, displacements and strains may be written in terms of displacements as $\mathbf{d} = \mathbf{H}D$ and $\boldsymbol{\varepsilon} = \mathbf{B}\mathbf{D}$, so that from Eq. (12):

$$\mathbf{K}D = \mathbf{F}; \quad \mathbf{K} = \sum_i \mathbf{K}_i \quad \mathbf{K}_i = \int_{V_i} B^T C_i B \, dV \tag{13}$$

being $\mathbf{K}$ the frame structural matrix, a sum of matrices $\mathbf{K}_i$ from the regions constructed with different materials. This matrix depends on the interpolation matrix $\mathbf{B}$ for the strain field. The discretized force vector $\mathbf{F} = \int_L \mathbf{H}^T \boldsymbol{\lambda} \, dl$ depends on the interpolation matrix for displacement field.

### 2.5 Results

The frame response to the considered loading was obtained running the finite element model in a comparative basis. The response of the plane running on fossil fuel against the one on hydrogen. Even though the framing is the same, loading is not. Inclusion of the proton exchange hydrogen fuel stack in place of the Citroen Visa engine, leads to changes in power and weight. Fuel tanks are quite distinct in size, position and weight as well.

Flexibility of the wing may be measured by the overall displacement field. In figure 5 this field is presented, assuming fixed-free conditions. Powertrain exchange changed the loading of the wings. At the same level flight now the airplane requires more lifting, translated into higher wing pressure. This entails higher tip wing deflections.

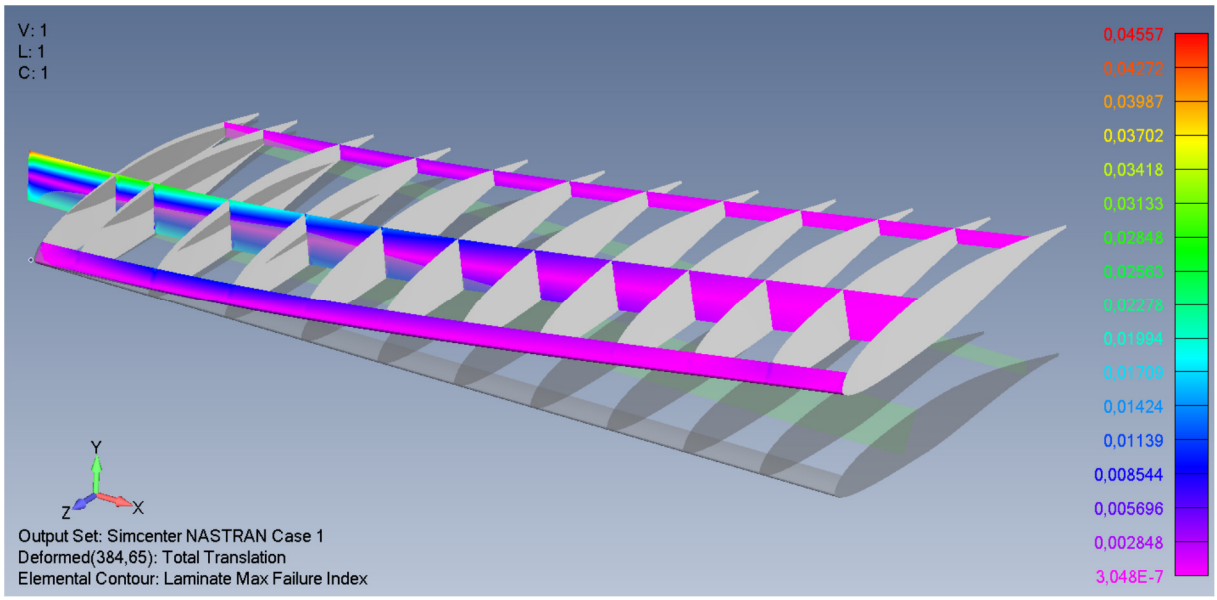


Figure 5. Lateral displacement field observed in the wing frame

When the plane was running on gasoline, the lift in each main wing was $L_w$. When running on hydrogen, it becomes $L_w + \Delta L_w$, due to change of total mass of the airplane from $m$ to $m + \Delta m$. This increment of lift generates an increase in the restraining force at the wing=fuselage interface equal to $\Delta L_w$ and an increase in fixing bending moment $\Delta L\,{}^{1}\!/_{4}$. Maximum stress and displacements in the wing suffered increases of:

$$\Delta\sigma_M = \frac{\Delta M}{W} \tag{14}$$

Being $W$ the sectional modulus. Increment in tip displacement is computed from:

$$\Delta v_m = {}^{1}\!/_{48}\,\Delta L_w b^3 \tag{15}$$

These increments are of the order of the increment of mass. Here $b$ is the semi-wing length. Reinforcement of the

wing is required when the powertrains is changed as safety factor of PIK wings is small.

Discretization and analysis of the fuselage under the same conditions was implemented as a separate part. In this form, lift and weight from the wings $R_w = L_w - W_w$, as well as empennage elements $R_e = L_e - W_e$ were applied to the fuselage. Bending moments from each side, along z axis ahead, equilibrate each other. Drag was set to equilibrate the thrust at the level flight. Figure 6 shows the weight distribution in the fuselage due to the change of power in the airplane.

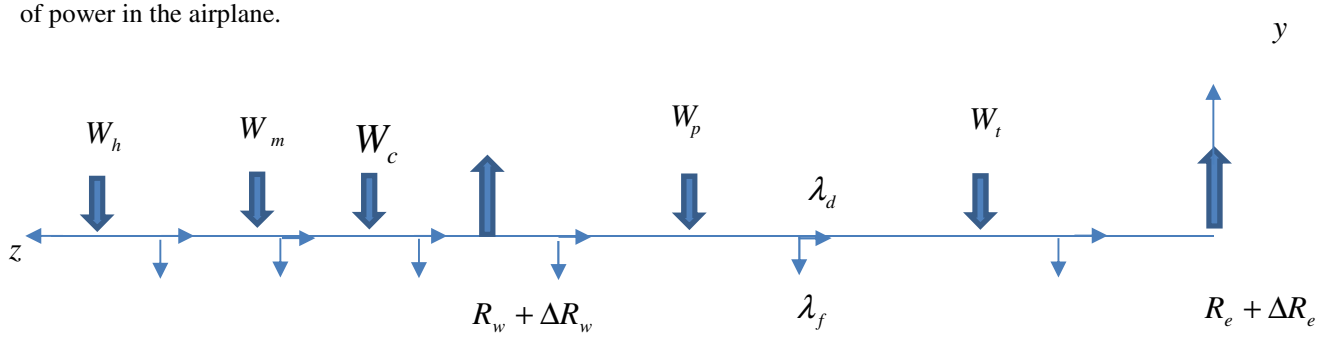


Figure 6: Schematics of the loading acting along the fuselage

Power system for fuel cell of weight $W_c$, with auxiliary systems and battery installed at $z_c$ with electric motor $W_m$ placed at $z_m$, before propeller $W_h$ at the end of fuselage $l_a$ stands ahead of wing spar fixing point, position $z_w$ where resultant $R_w$ appears. Prior to this position, pilot $W_p$ at $z_p$ and hydrogen fuel tank $W_t$ at $z_t$ are installed. Empenage of lateral resultant $R_e$ appear at origin z=0. Trim of the airplane stablishes some these values, if no ballast is used. Balance moment from propeller $W_h\Delta$ completes the load distribution. Distribute loading includes the drag $\lambda_D$ and fuselage weight $\lambda_f$ both per unit length. Internal efforts, normal $N$, shear $S$ and bending moment $M$ in each interval $i = 1,2,..,n$ will give, in recursive form:

$$N = N_{i-1} + \int_{z_i}^{zz} \lambda_D dz \tag{16}$$

$$S = S_{i=1} + W_i + \int_{z_{i-1}}^{z} \lambda_f dz \tag{17}$$

$$M = M_{i=1} - S_{i-1}(z - z_{i-1}) - W_{i-1}(z - z_{i-1}) = \int_{z_{i-1}}^{z} \lambda_f (z - z')dz' \tag{18}$$

All elements of the old and new power source were arranged in a symmetrical manner around the main symmetry plane of the PIK 26. Fuel tank was placed at the tail region, connected to the hydrogen line and fuel cell, both placed just ahead of the cockpit of pilot. Electronics and battery were arranged around this same position. Battery, admission line system and electrical motor were placed in the front region. Before change of power, all mechanical elements were placed in different positions $z_i$ .

Drag and lift suffer increments $\Delta D$ and $\Delta L$ in level flight when powertrain changed. Internal efforts in each transverse section of the fuselage suffer increments $< \Delta N, \Delta S, \Delta M >$. They give rise to increments in the associated values of stress at every section z:

$$\Delta\sigma_N = \frac{\Delta N}{A}; \quad \Delta\tau = \kappa\frac{\Delta S}{A}; \qquad \Delta\sigma_M = \frac{\Delta M}{\mathcal{W}} \tag{19}$$

Increments on $\sigma_N, \tau_S, \sigma_M$ occur in each and every point of the section. In particular at the critical point of each section. And mostly in the critical section of the fuselage.

The increase on values of stress from one and to the other power condition, were differentiated by the distribution and increased loading. In Figure 7, the finite element model of the fuselage for the internal combustion engine is presented. The region of fixation of wing to the fuselage, shows points requiring detailed discretization for they are in the verge of inelastic strains. Under new power should present large amounts of permanent strain. This means that reinforcement in the fuselage is necessary if the fuel change is implemented. The finite element results corroborate this for the failure index. Use of another arrangement, metal or composite material are possible means of solving this problem.

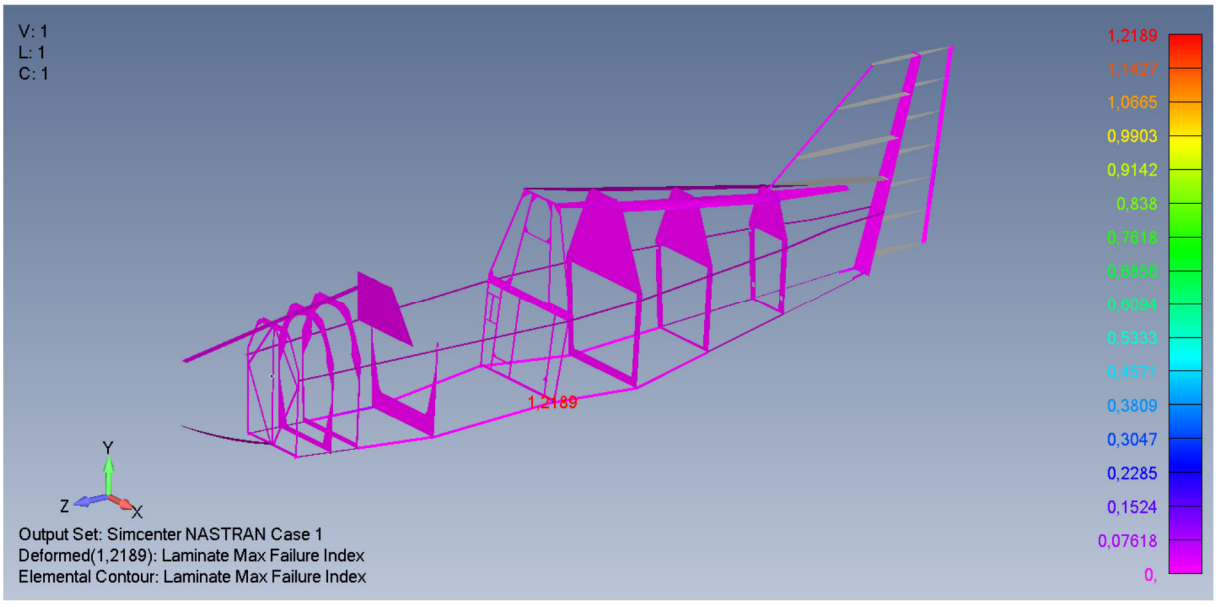


Figure 7: Stress field in the fuselage frame of PIK 26

### 3. Conclusions

The decision of avoiding fossil fuel, without using solar panels, had an appeal as possibly only small changes in the form, size and arrangement of components in a fossil fuel airplane could solve satisfactorily the problem. The choice of a simple and very light plane was considered the natural choice. Fixed the same mission requirements, the amount of additional weight and power required from the new system, made part of this hypothesis inaccurate.

The structure of PIK 26 does not have a very large degree of redundancy, and cannot accommodate the increase of weight and power required without reinforcement of the structure, be it by means of use of composite materials in its construction, be with local reinforcement of critical regions of the structure.

**Authorship statement.** The authors hereby confirm that they are the sole liable persons responsible for the authorship of this work, and that all material that has been herein included as part of the present paper is either the property (and authorship) of the authors, or has the permission of the owners to be included here.

## References

[1] T. R. Yechout et all, Introduction to Aircraft Flight Mechanics, AIAA Educational Series, 2010
[2] Isadora F. Tacksian. Avião Experimental PIK26 :Desenho, Modelo e Análise, IC 2021, UFABC, Brazil
[3] Pei-Hsiang, et all, Design, Manufacturing and Fligth Testing of an Experimental Flying Wing UAV, Applied Sciences, 2019, vol.9, 3043
[4] Mark Schmelcher and Jannik, Haay, Hydrogen Fuel Cells for Aviation?, ISABE, 2022
[5] XFLR5 program, http://www.xflr5.tech/xflr5.htm
[6] G.L.M. Vonhoff, Conceptual Design of Hydrogen Fuel Cell Aircraft, TUDelft, MS.C. Thesis, 2021
[7] https://horizoneducacional.com: 65 KW Liquid Cooled Fuel Cell
[8] MSC-Nastran, 2022, https://en.wikipedia.org/wiki/Nastran